Structural Study of the Solid-State Photoaddition Reaction of Arylidenoxindoles

Marco Milanesio

Dipartimento di Chimica IFM, Università, Via P. Giuria 7, I-10125 Torino, Italy

Davide Viterbo*

Dipartimento di Scienze e Tecnologie Avanzate, Università del Piemonte Orientale "A. Avogadro", Corso T. Borsalino 54, I-15100 Alessandria, and Dipartimento di Chimica IFM, Università, Via P. Giuria 7, I-10125 Torino, Italy

Angelo Albini* and Elisa Fasani

Dipartimento di Chimica Organica, Università, Via Taramelli 10, I-27100 Pavia, Italy

Riccardo Bianchi and Mario Barzaghi

Centro di Studio per le Relazioni tra Struttura e Reattività Chimica, CNR, Via C. Golgi 19, I-20133 Milano, Italy

Received December 6, 1999

The photochemistry of isomeric 2-furyliden- and benzylidenoxindoles (2*H*-indol-2-ones) is examined. In solution *E*−*Z* isomerization is the only process via the excited singlet state (which fluoresces in glassy solution at 77 K and not at room temperature). In the crystalline state, the two *(Z)* derivatives are photostable, in accordance with the prediction based on the structural determination of the furylidene derivative, which adopts the unreactive Schmidt's γ type arrangement. The *(E)* furylidene derivative (**1a**) gives efficiently ($\Phi = 0.3$) the head-to-tail dimer, as indicated by the crystal structure, which is of the reactive α type, in full accord with the topochemical principles. In contrast, the corresponding benzylidene (**1b**) derivative reacts sluggishly ($\Phi < 0.01$) and mainly gives polymers, despite the fact that crystal structure determination shows that it likewise pertains to the α type and complies with the topochemical rules. The difference in reactivity is explained on the basis of (i) the twist of the phenyl ring with respect to the indole plane, and (ii) the higher overall cohesion energy and the lower interaction energy between facing molecules, as found from the charge density analysis for the crystals of **1b** in comparison to those of **1a**. This evidences a further stringent requirement for the occurrence of topochemical photodimerizations.

Introduction

Organic reactions in the crystalline state have been known for more than a hundred years, and among them photodimerizations have received considerable attention. A major contribution to the understanding of the requirements needed to realize these reactions in the solid state came from the work of Schmidt and co-workers,[1] who established the fundamental topochemical rules. The basic assumption of these rules is that the arrangement of the molecules in the crystal lattice determines the result, in the sense that only molecules arranged in such a way that the formation of the new bonds requires a minimal motion react and the regio- and sterochemistry of the cycloadducts reproduces the preexistent arrangement in the crystal. The typical example is that of the different crystalline forms of cinnamic acids giving different [2 + 2] photocycloadducts. Schmidt's geometrical rules were validated by a rather large number of studies on photocycloaddition reactions.[2] The most convincing evidence of the validity of the topochemical rules came from the studies of a small number of single crystal to single crystal reactions.[3−5] At the same time, over the years, exceptions to the rules were also found, i.e., products expected to react did not react at all or gave the "wrong" cycloadduct, while molecules in unsuitable topochemical positions in the crystal reacted. In an attempt at explaining these exceptions Kaupp[6] interpreted his AFM experiments in terms of significant mass displacements at the crystal surface contradicting the topochemical postulate of minimal motion. Heterogeneous surface transformations may well occur with mass transport and phase separation, and this type of mechanism can possibly explain some of the cases when the reaction takes place in absence of topochemical prerequisites, but it is unable to account for the more frequent cases of nonreactive crystals complying with the rules.

(1) Cohen, M. D.; Schmidt, G. M. J.; Sonntag, F. I. *J. Chem. Soc.* **1964**, 2001−2013. Schmidt, G. M. J. *J. Chem. Soc.* **1964**, 2014−2021.

(2) Ramamurthy, V.; Venkatesan, K. *Chem. Rev.* **1987**, *87*, 433−481. Garcia-Garibay, M. A.; Constable, A. E.; Jernelius, J.; Choi, Y.; Cizmeciyan, D.; Shin, S. H. In *Physical Supramolecular Chemistry*; Echegoyen, L., Kaifer, A. E., Eds.; Kluwer Academic Press: Dordercht, 1996; pp 289−312. Kaupp, G. In *Organic Photochemistry and Photobiology*; Horspool, W. M., Song, P. S., Eds.; CRC: Boca Raton, 1995; pp 50−63.

(3) Novak, K.; Enkelmann, V.; Wegner, G.; Wagener, K. B. *Angew. Chem., Int. Ed. Engl.* **1993**, *32*, 1614−1616.

(4) Enkelmann, V.; Wegner, G.; Novak, K.; Wagener, K. B. *J. Am. Chem. Soc.* **1993**, *115*, 10390−10391.

(5) Köhler, W.; Novak, K.; Enkelmann, V. *J. Chem. Phys.* **1994**, *101*, 10474−10480.

(6) Kaupp, G. *Angew. Chem., Int. Ed. Engl.* **1992**, *31*, 592−598.

10.1021/jo991873i CCC: $19.00
Published on Web 05/11/2000

Scheme 1

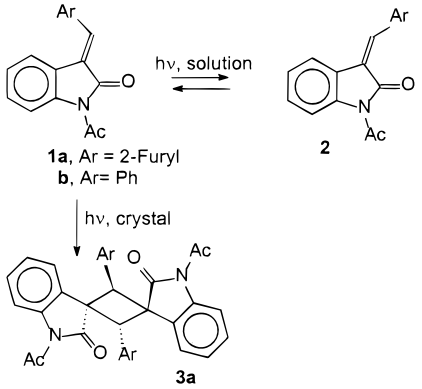

We report here some results on the solid-state reactivity of some (hetero)arylidenoxindoles. These can be considered as derivatives both of cinnamic acid and of stilbene, i.e., of the two main classes of compounds known to photodimerize, with the so far scarcely investigated additional feature of a further conjugated substituent[7,8] at the supposedly reactive C=C double bond (cf. Scheme 3). This crowding around the reactive center was expected to be informative of the requisites for photoreaction. As it will appear in the following, the photochemical behavior was in fact quite structure-dependent, and we feel that our results offer further insight into the mechanism of solid-state photodimerization.

Results

(Hetero)arylidenoxindoles are conveniently obtained by condensation of oxindole with the appropriate aldehyde (see the Experimental Section). A mixture of geometric isomers is obtained and can be separated. The compounds were acetylated to avoid a directing effect that the N−H bond had on the molecular packing. In this work, we considered the *(Z)* and *(E)* isomers of *N*-acetyl 2-furylidene- and 2-benzylidenoxindoles **1** and **2** (see Scheme 1).

Photochemical Studies in Solution. Irradiation of the above oxindoles in solution (benzene, acetonitrile, or chloroform) led in every case to rapid *E*−*Z* interconversion (**1** → **2** and vice versa). In every case a close to 1:1 steady-state mixture was obtained by irradiation with Pyrex-filtered light. The quantum yield for the **1a** → **2a** isomerization was 0.4, and the other isomerizations occurred at a similar rate. Prolonged irradiation led to the formation of small amounts of different products, some of which corresponded to those obtained in the solid state and identified as dimers (see below).

None of these oxindoles showed a detectable fluorescence in solution. On the other hand, emission was readily observed in a glassy matrix at 77 K (Figure 1, dotted line) and was recognized as fluorescence, since it was not detected when a phosphoroscope was used.

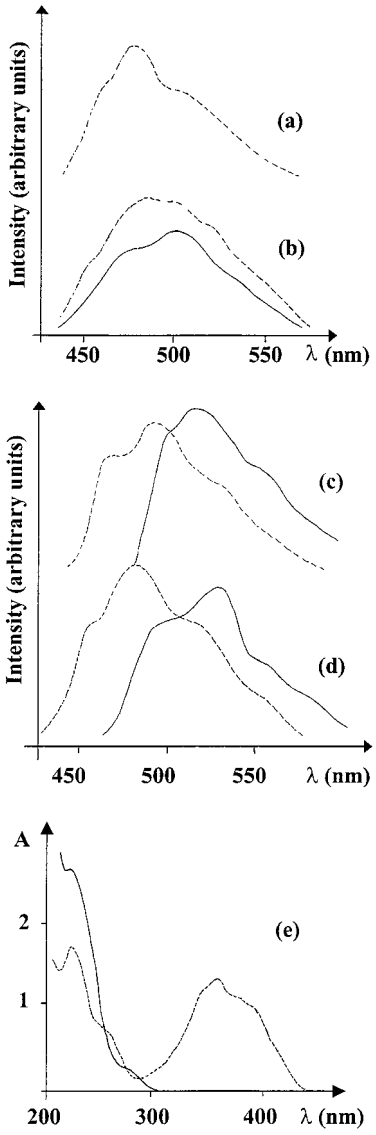

Figure 1. Emission spectra of arylidenoxindoles **1** and **2** by irradiation at 360 nm in EPA glass at 77 K (dotted line) and in the crystalline state (continuous line): (a) **1a**, (b) **1b**, (c) **2a**, (d) **2b**, and absorption spectra (e) of arylidenoxindole **1a** (1×10^{-4} M, dotted line) and of dimer **3a** (5×10^{-5} M, continuous line) in MeCN at room temperature.

Photochemical Studies of 1a in the Solid State. In the solid state the *(E)*-furylidene derivative **1a** was highly photoreactive. This compound formed large yellow needles that, when exposed to a lamp emitting in the near UV or to solar light, reacted in a few hours. The large crystals "burst", scattering around fragments for several centimeters. Observation under the microscope showed that the crystal cracked perpendicularly to the elongation axis, corresponding to the short *b* axis (cf. Table 1). The reaction could be conveniently carried out by grinding the crystals and shaking them from time to time to change the exposed surface. Under these conditions gram samples of **1a** could be easily brought to ≥85% conversion in a few hours by means of a mercury arc. The material was purified by recrystallization and recognized to be the head-to-tail cyclobutane dimer **3a** on the basis of the spectroscopic features and the single-

(7) Intramolecular crystal state cycloadditions involving trisubtituted C=C double bonds, with the third one being a nonconjugating, usually an alkyl group, are largely known and include cases where the double bond is exo to a ring, showing that purely steric crowding is not per se a limitation. See, e.g., refs 7 and 8: Nakanishi, H.; Jones, W.; Thomas. J. M.; Hursthouse, M. B.; Motevalli, M. *J. Phys. Chem.* **1981**, *85*, 3636−3642. Jones, W.; Ramdas, S.; Theocaris, C. R.; Thomas, J. M.; Thomas, N. W. *J. Phys. Chem.* **1981**, *85*, 2594−2597. Kearsley, S. K.; Desiraju, G. R. *Proc. R. Soc. London, Ser. A*, **1985**, *397*, 157−181. Rabinovitch, D.; Schmidt, G. M. J. *J. Chem. Soc. B* **1967**, 144−149. Kaupp, G.; Jostkleigrewe, E.; Hermann, H. J. *Angew. Chem., Int. Ed. Engl.* **1982**, *21*, 435−436. Chase, D. B.; Amey, R. L.; Holtje, W. G. *Appl. Spectrosc.* **1982**, *36*, 155−158. Waschen, E.; Mantsch, R., Krampity, D, Hartke, K. *Liebigs Ann. Chem.* **1976**, 2137−2144.

(8) Theocaris, C. R.; Jones, W.; Thomas, J. M.; Motevalli, M.; Horsthouse, M. B. *J. Chem. Soc., Perkin Trans. 2* **1984**, 71−76.

Table 1. Crystal Data and Structure Refinement for Compounds 1a, 1b, 2a, and 3a

	1a	1b	2a	3a
		Crystal Data		
empirical formula	$C_{15}H_{11}NO_3$	$C_{17}H_{13}NO_2$	$C_{15}H_{11}NO_3$	$C_{30}H_{22}N_2O_6$
rormula weight	253.25	263.28	253.25	506.50
crystal system	monoclinic	monoclinic	monoclinic	monoclinic
space group	P2/n	$P2_1/c$	$P2_1/c$	$C2/c$
unit cell dimensions	$a = 12.006(1)$ Å	$a = 8.099(1)$ Å	$a = 4.585(3)$ Å	$a = 14.961(2)$ Å
	$b = 5.523(1)$ Å	$b = 9.299(1)$ Å	$b = 17.699(12)$ Å	$b = 12.563(2)$ Å
	$c = 18.407(2)$ Å	$c = 17.511(2)$ Å	$c = 14.904(7)$ Å	$c = 12.779(2)$ Å
	$\beta = 104.30(1)°$	$\beta = 97.95(1)°$	$\beta = 91.02(5)°$	$\beta = 94.18(1)°$
volume	1182.7(3) Å^3	1306.1(3) Å^3	1209.3(13) Å^3	2395.5(6) Å^3
Z	4	4	4	4
density (calculated)	1.422 Mg/m^3	1.339 Mg/m^3	1.391 Mg/m^3	1.404 Mg/m^3
absorption coefficient	0.100 mm^{-1}	0.088 mm^{-1}	0.098 mm^{-1}	0.099 mm^{-1}
F(000)	528	552	528	1056
crystal size (mm)	0.30 × 0.35 × 0.45	0.40 × 0.58 × 0.86	0.60 × 0.21 × 0.18	0.22 × 0.38 × 0.64
		Data Collection		
θ range for data collection	1.84° to 27.57°.	2.49° to 35.03°.	1.79° to 22.51°.	2.12° to 25.00°.
index ranges	$0 \le h \le 15$,	$-3 \le h \le 13$,	$-4 \le h \le 4$,	$0 \le h \le 17$,
	$0 \le k \le 7$,	$-15 \le k \le 14$,	$0 \le k \le 19$,	$0 \le k \le 14$,
	$-23 \le l \le 23$	$-28 \le l \le 28$	$0 \le l \le 15$	$-15 \le l \le 15$
reflections collected	2833	6101	2419	2175
independent reflections	2692 with $R(\text{int}) = 0.0212$	5677 with $R(\text{int}) = 0.0219$	1555 with $R(\text{int}) = 0.0907$	2094 with $R(\text{int}) = 0.0498$
completeness	98.5%	99.0%	98.9%	98.8%
		Refinement		
data/parameters	2692/216	5677/233	1555/172	2094/216
goodness-of-fit on F^2	1.022	1.006	1.043	1.003
final R indices [$I > 2\sigma(I)$]	R1 = 0.0404,	R1 = 0.0517,	R1 = 0.0894,	R1 = 0.0587,
	wR2 = 0.0943	wR2 = 0.1283	wR2 = 0.2130	wR2 = 0.1293
R indices (all data)	R1 = 0.0688,	R1 = 0.0837,	R1 = 0.1776,	R1 = 0.1151,
	wR2 = 0.1085	wR2 = 0.1469	wR2 = 0.2686	wR2 = 0.1584
largest diff. peak and hole	0.214 and −0.188 e Å^{-3}	0.459 and −0.234 e Å^{-3}	0.243 and −0.470 e Å^{-3}	0.239 and −0.287 e Å^{-3}

crystal structure determination. NMR analysis showed that no other photoproduct was present in the reaction mixture in a significant amount.

The reaction could be monitored by various techniques. Irradiation of a sample in a KBr pellet could be followed until the IR absorption bands typical of the starting material could no longer be detected, indicating that the conversion was ≥85−90%. The shift of the C═O absorption bands from 1695 and 1740 to 1710 and 1760 cm^{-1} (compare Figure 2a and 2b) were a clear indication that reaction had taken place at the conjugated C═C double bond. In fact, the spectrum obtained (Figure 2b) was identical to that of recrystallized **3a** (Figure 2c) in the 1800−1300 cm^{-1} but showed some small differences in the C−H stretching band at ca. 3100 cm^{-1} and in the region 1300−500 cm^{-1}, although the general pattern was the same.

Under this condition the rate of the reaction was 60% of that of the photorearrangement of *o*-nitrobenzaldehyde to *o*-nitrosobenzoic acid.[9] Since a quantum yield of 0.5 has been reported for the latter reaction in the solid state and the KBr pellets were prepared in the same way so that the fraction of scattered light was reasonably the same, we inferred that the photodimerization of **1a** occurs with a quantum yield of 0.3.

Powder diffraction experiments on ground crystalline samples that had been exposed for different irradiation times (with occasional shaking during the prolonged irradiation) showed that the starting material was consumed up to about 85%, while a new set of reflections developed (see Figure 3). The position and intensity of these reflections differed from those calculated from the crystal structure of recrystallized **3a** (Figure 7). The difference in the diffraction patterns, together with the above-mentioned minor differences in the IR spectrum, indicated that the "as formed" substance was a polymorph of the recrystallized sample (NMR spectra of the dissolved samples confirmed the conversion into **3a**). Indeed, after washing the resulting powder with a little chloroform to take away unreacted **1a**, partial recrystallization of **3a** took place and was revealed by the appearance of the expected reflections in the diffraction pattern.

Photochemical Studies in the Solid State of the Other Oxindoles. The crystalline *(Z)* furylidene derivative **2a** was much more photostable. After 7 days of irradiation only tiny amounts of new products were present. The NMR spectrum of the mixture was compatible with the formation of the four possible cyclobutane dimers (two of them in a larger proportion), although the overall conversion remained low (about 10%).

The *(E)* benzylidene derivative **1b** was also rather stable. Prolonged irradiation gave a highly insoluble material. A part of the irradiated solid could be extracted with DMSO and was shown to consist of unchanged **1b** along with 25% of different products, reasonably a mixture of the four possible dimers. As for the non-extracted material, the displacement of the C═O IR absorption bands was consistent with saturation of the double bond, and therefore we assumed that this was a polymer resulting from addition at that bond (tentative

(9) Kuhn, H. J.; Braslavsky, S. E.; Schmidt, R. *Pure Appl. Chem.* **1989**, *61*, 187.

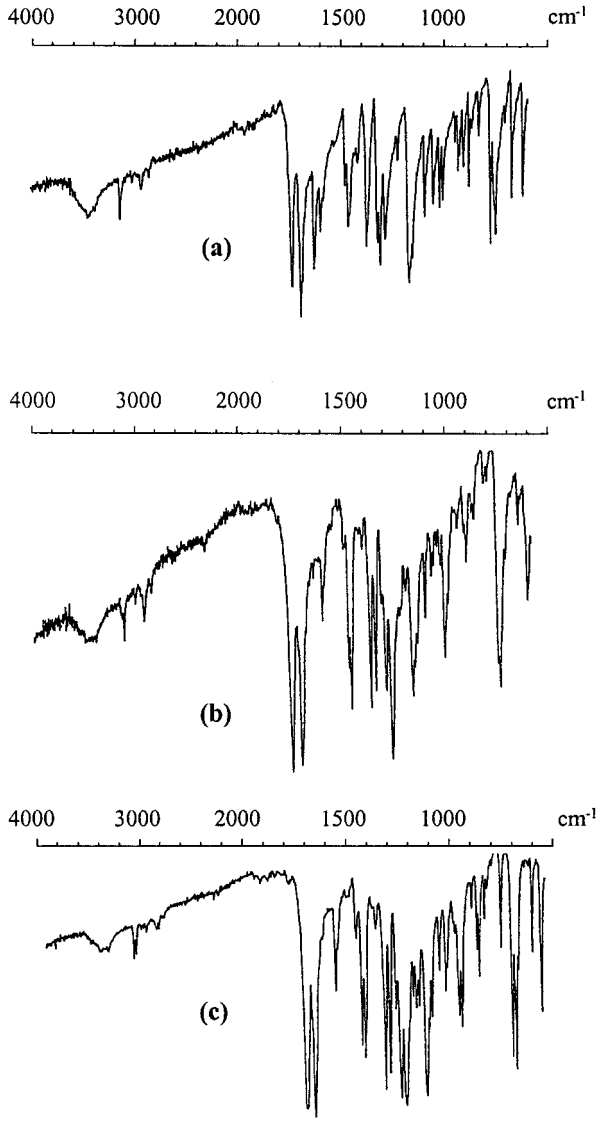

Figure 2. (a) IR spectrum of a dispersion of furylidenoxindole **1a** in KBr. (b) IR spectrum of the same KBr pellet irradiated until ca. 85% conversion of **1a** had been reached (see Experimental Section). (c) IR spectrum of a recrystallized sample of the dimer **3a** (see Experimental Section).

Scheme 2

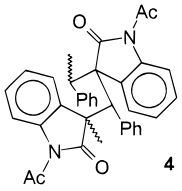

4

structure, **4** in Scheme 2). The corresponding *(Z)* isomer **2b** was essentially photostable in the solid state.

Comparison with *o*-nitrobenzaldehyde in KBr showed that with all of the above oxindoles the quantum yield for photoreaction was $\ll 10^{-2}$.

In the crystalline state, both *(Z)* derivatives **2a** and **2b** exhibited an intense yellow emission, which was 30−40 nm red-shifted with respect to the luminescence observed in ether/pentane/ethyl alcohol 5/5/2 (EPA) glass (see Figure 1). With the *(E)* derivative **1b** the luminescence was weaker and practically unshifted, while no emission was detected from crystalline **1a**.

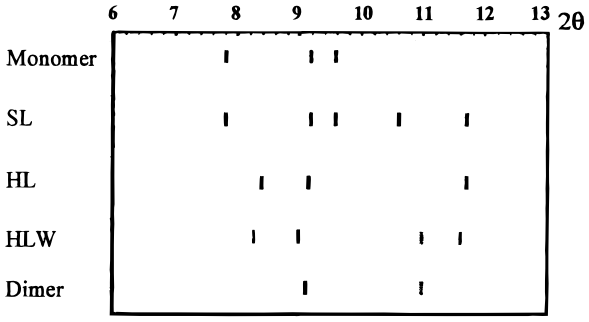

Figure 3. Comparison of the powder diffraction patterns of **1a** and of its photoreaction products obtained under different conditions, using Cu Kα X-ray radiation. Only the 2*θ* positions of the diffraction lines are shown. *SL* indicates the sample exposed to two 15 W, 360 nm phosphor-coated lamps for 1 h; *HL* is the sample exposed for 10 h (with occasional shaking); and *HLW* is the same *HL* sample but after washing with chloroform.

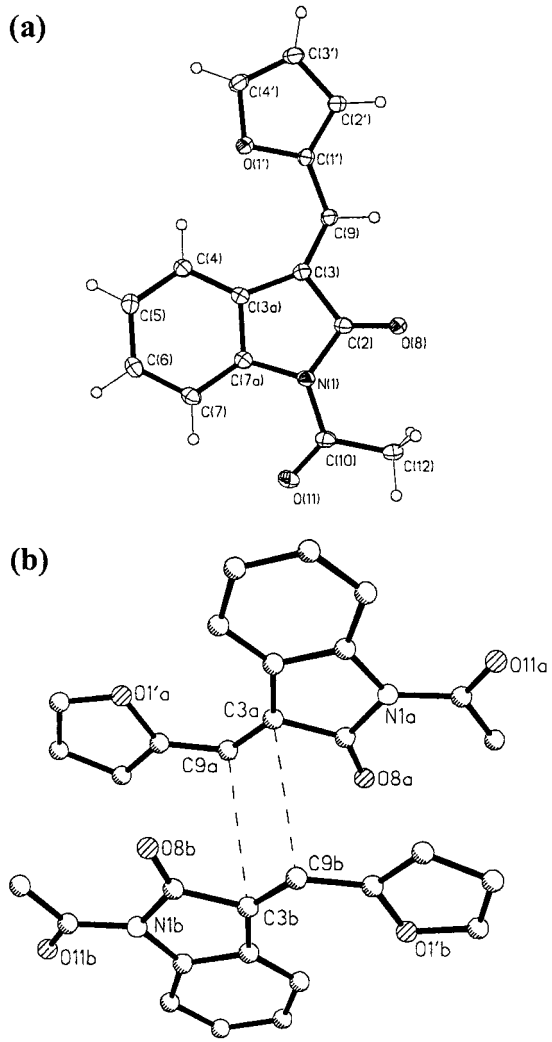

Figure 4. (a) Drawing of the molecular structure of compound **1a**, showing the adopted labeling scheme, with displacement ellipsoids drawn at the 30% probability level. (b) Drawing of the two facing and potentially reactive molecules in the **1a** crystal.

Crystal Structures. We have solved the crystal structures of the two *(E)* furylidene and benzylidene derivatives **1a** and **1b**, of the *(Z)* furylidene derivative **2a** [the *(Z)* benzylidene derivative **2b** did not give suitable

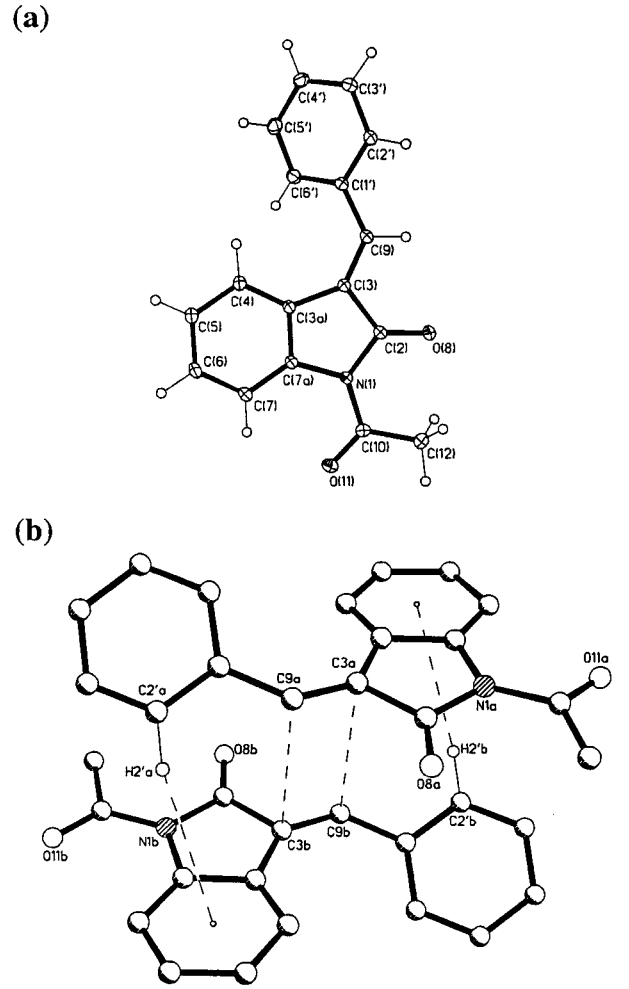

Figure 5. (a) Drawing of the molecular structure of compound **1b**, showing the adopted labeling scheme, with displacement ellipsoids drawn at the 30% probability level. (b) Drawing of two facing and potentially reactive molecules in the **1b** crystal.

crystals], and of the furyl dimer **3a**. These structures are shown in Figures 4a, 5a, 6a, and 7, while Figures 4b, 5b, and 6b show the facing of pairs of potentially reactive monomers. The most relevant bond distances are listed in Table 3 for all derivatives.

The molecule of the *(E)* furylidene derivative **1a** was almost planar (dihedral angle between the furyl and the oxindole planes, 7.6°) in keeping with a π delocalization of the stylbene type involving both ring systems through the C3=C9 double bond. This type of conjugation was confirmed by the trend of bond distances given in Table 3. The small twist angle indicated that the five-membered ring was well accommodated in the molecule without relevant steric hindrance. In the crystal the molecules were held together by van der Waals forces and by weak C−H···O intermolecular interactions (C2′−H···O8: C2′···O8 = 3.227 Å, H···O8 = 2.34 Å; C6−H···O11: C6···O11 = 3.431 Å, H···O11 = 2.50 Å).

Instead, the molecules of the *(E)* benzylidene derivative **1b** (Figure 5a) were not planar, and the phenyl ring was rotated by 38.9° with respect to the oxindole moiety. The stylbene-type π delocalization was thus reduced (but not wholly canceled) as shown by the significant lengthening of the C9−C1′ bond distance (cf. Table 3) with respect to **1a**. As in **1a** the molecules in the **1b** crystal were held

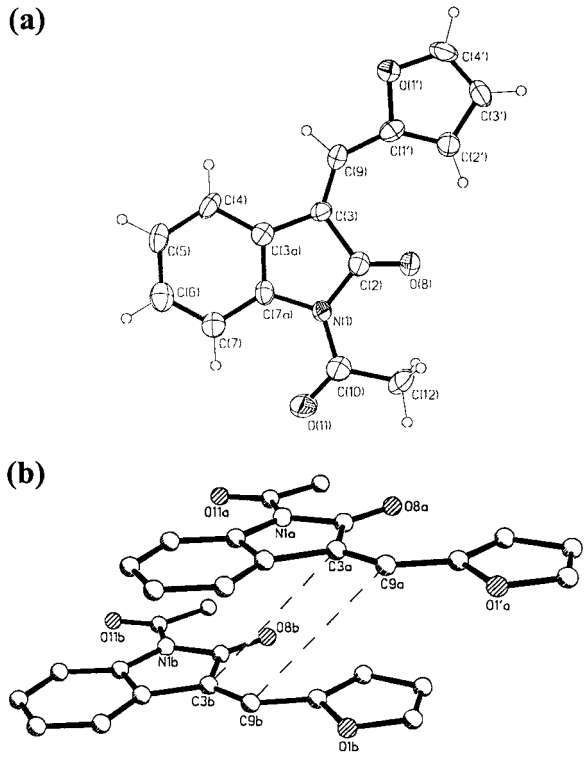

Figure 6. (a) Drawing of the molecular structure of compound **2a**, showing the adopted labeling scheme, with displacement ellipsoids drawn at the 30% probability level. (b) Drawing of two facing and potentially reactive molecules in the **2a** crystal.

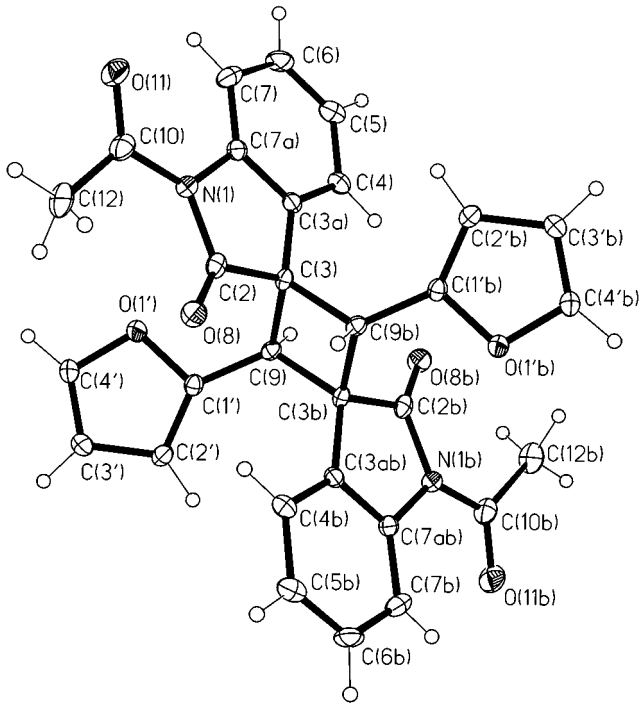

Figure 7. Drawing of the molecular structure of compound **3a**, showing the adopted labeling scheme, with displacement ellipsoids drawn at the 30% probability level.

together only by van der Waals and weak C−H···O interactions (C6−H···O11: C6···O11 = 3.392 Å, H···O11 = 2.41 Å).

The molecules of the *(Z)* furylidene derivative **2a** (Figure 6a) were also planar (dihedral angle between the

Table 2: Values of the Most Relevant Geometrical Parameters Foreseen by the Topochemical Rules for 1a and 1b[a]

	1a	1b	ideal
θ_1 (deg)	0.0	0.0	0.0
θ_2 (deg)	92.0	95.1	90.0
θ_3 (deg)	115.0	111.2	90.0
center-to-center distance (Å)	3.498	3.877	<4.2
D_1 (Å)	0.175	0.384	0.0

[a] As illustrated in ref 2 (Figure 5, page 440) by Ramamurthy and Venkatesan.

Table 3. Selected Bond Lengths (Å), Angles (deg), and Torsion Angles (deg) for 1a, 1b, 2a, and 3a

	1a	1b	2a	3a
		Bond Lengths		
N(1)−C(10)	1.405(2)	1.403(1)	1.417(9)	1.406(5)
N(1)−C(2)	1.422(2)	1.422(1)	1.405(9)	1.407(4)
N(1)−C(7a)	1.427(2)	1.427(1)	1.422(8)	1.441(4)
C(7)−C(7a)	1.383(2)	1.391(1)	1.381(10)	1.387(5)
C(3a)−C(7a)	1.412(2)	1.402(1)	1.385(10)	1.391(5)
C(3a)−C(4)	1.394(2)	1.393(1)	1.381(10)	1.384(5)
C(3)−C(3a)	1.460(2)	1.459(1)	1.466(10)	1.495(4)
C(4)−C(5)	1.391(2)	1.394(1)	1.382(10)	1.394(5)
C(5)−C(6)	1.386(2)	1.391(2)	1.378(12)	1.373(6)
C(6)−C(7)	1.392(2)	1.396(2)	1.382(11)	1.391(5)
C(3)−C(9)	1.352(2)	1.348(1)	1.337(10)	1.580(4)
C(2)−C(3)	1.490(2)	1.490(1)	1.510(10)	1.522(4)
C(2)−O(8)	1.209(2)	1.210(1)	1.204(8)	1.201(4)
C(9)−C(1′)	1.424(2)	1.462(1)	1.431(10)	1.483(4)
C(10)−O(11)	1.212(2)	1.212(1)	1.205(9)	1.220(4)
C(10)−C(12)	1.495(3)	1.495(2)	1.466(10)	1.484(6)
C(3)−C(9b)				1.572(4)
		Bond Angles		
C(10)−N(1)−C(2)	126.0(1)	126.2(1)	125.7(6)	125.5(3)
C(10)−N(1)−C(7a)	124.6(1)	124.7(1)	123.9(7)	109.3(3)
C(2)−N(1)−C(7a)	109.2(1)	109.0(1)	110.3(6)	124.8(3)
C(7)−C(7a)−C(3a)	121.6(1)	121.5(1)	120.6(7)	122.1(3)
C(7)−C(7a)−N(1)	128.9(1)	128.8(1)	130.2(7)	128.5(3)
C(3a)−C(7a)−N(1)	109.5(1)	109.6(1)	109.1(6)	109.3(3)
C(4)−C(3a)−C(7a)	119.2(1)	119.7(1)	121.1(7)	120.3(3)
C(4)−C(3a)−C(3)	132.9(1)	131.9(1)	129.7(7)	129.8(3)
C(7a)−C(3a)−C(3)	107.9(1)	108.1(1)	109.2(6)	109.8(3)
C(5)−C(4)−C(3a)	119.1(1)	119.3(1)	118.3(8)	118.0(3)
C(6)−C(5)−C(4)	120.8(2)	120.1(1)	120.4(8)	120.9(4)
C(5)−C(6)−C(7)	121.1(2)	121.5(1)	121.6(8)	122.1(3)
C(7a)−C(7)−C(6)	118.1(1)	117.7(1)	118.0(8)	116.5(3)
C(9)−C(3)−C(3a)	136.8(1)	135.7(1)	127.2(7)	116.0(3)
C(9)−C(3)−C(2)	116.4(1)	117.9(1)	127.7(7)	114.0(3)
C(3a)−C(3)−C(2)	106.7(1)	106.4(1)	105.1(6)	103.3(3)
O(8)−C(2)−N(1)	125.8(1)	125.7(1)	127.2(7)	126.4(3)
O(8)−C(2)−C(3)	127.6(1)	127.7(1)	126.3(7)	125.4(3)
N(1)−C(2)−C(3)	106.7(1)	106.6(1)	106.3(6)	108.2(3)
C(3)−C(9)−C(1′)	132.9(1)	130.4(1)	132.0(7)	117.7(3)
O(11)−C(10)−N(1)	119.6(2)	119.5(1)	119.4(7)	119.2(4)
O(11)−C(10)−C(12)	122.1(1)	122.1(1)	121.5(8)	123.2(4)
N(1)−C(10)−C(12)	118.3(1)	118.4(1)	119.1(8)	117.6(3)
C(3)−C(9)−C(3b)				91.5(2)
C(9)−C(3)−C(9b)				88.5(2)
C(2′)−C(9)−C(3b)				120.6(3)
C(3a)−C(3)−C(9b)				123.9(3)
C(2)−C(3)-C(9b)				111.3(3)
		Torsion Angles		
C(3)−C(9)− C(1′)−C(2′)	179.7(2)	152.3(1)	2.0(2)	−133.1(4)
C(3a)− C(3)− C(9)−C(1′)	2.9(3)	−7.7(2)	177.4(8)	−106.6(3)

furyl and the oxindole planes 1.4°) with the same degree of π delocalization as in **1a**.

The molecules of the furyl head−tail dimer **3a** (Figure 7) sat on a crystallographic inversion center coinciding with their center of mass in the middle of the cyclobutane ring. The four carbon atoms C3, C9, C3b, C9b of the ring, having now an sp^3 hybridization, could no longer contribute to the π delocalization, and the furyl and oxindole rings became independent aromatic systems. The cyclobutane ring was forced by symmetry to be planar but was not a regular square. The two sides were very similar [C3−C9 = 1.575(6) Å, C3−C9b = 1.579(6) Å], but the angle at C3 of 88.4° was significantly smaller than that at C9 of 91.6°. The furyl and the oxindole moieties stuck out of the cyclobutane plane, forming with it dihedral angles of 46.5° and 85.6° respectively. The dihedral angle between the furyl and the oxindole planes was 49.4°. The weak C−H···O intermolecular interaction (C4′−H···O8: C4′···O8 = 3.278 Å, H···O8 = 2.41 Å) was retained in the dimer.

Scheme 3

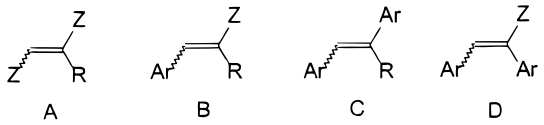

R=H, alkyl; Z= COOH, COOR, CONHR, CO,

Charge Density Calculations. On the low-temperature data of **1a** and **1b** we also carried out a charge density study with the aim also of evaluating the packing energies. A calculation of the molecular interaction energies, derived from the charge density analysis, showed that the cohesion energy was smaller (−3.0 kcal/mol) for **1a** than for **1b** (−5.0 kcal/mol), while the value of the interaction energy between pairs of facing (and potentially reactive) molecules (Figures 4b and 5b) was significantly greater (−4.0 kcal/mol) for **1a** than for **1b** (−1.0 kcal/mol).

Discussion

The photochemistry of oxindoles **1** and **2** in solution requires little comment, being just another case of photoinduced geometrical isomerization. The high rate of rotation around the exocyclic double bond precludes other excited-state processes such as emission and addition. The quantum yield of isomerization is 0.5 ± 0.1, as often observed for this kind of process,[10] and is independent from the presence of oxygen. When rotation is inhibited by viscosity in the glass at 77 K an intense fluorescence appears, while there is no phosphorescence. Thus, there is no evidence for the occurrence of a significant intersystem crossing to the triplet, and the isomerization appears to proceed from the singlet state.

Compound **1a** can be conveniently photodimerized in the solid state. As it appears from Figure 1e, the dimer is transparent in the wavelength range used, and thus the reaction proceeds until up to 85% of the starting material is consumed. As mentioned above, a rough evaluation of the quantum yield (taking *o*-nitrobenzaldehyde as an actinometer) shows that the dimerization is efficient ($\Phi \cong 0.3$). The different behavior of the four arylidenoxidoles examined deserves some discussion in the frame of the current rationalization on the topic.

The reported examples fall into three classes: fumaric acid derivatives (A), cinnamic acid derivatives (B), stilbenes (C). However, to our knowledge, no example where all three substituents at the C=C double bond have a conjugated multiple bond (type D) had been previously investigated.[7,8] The present study of a type D case shows a diversity of behaviors for the derivatives considered, from an efficient and selective dimerization to no reaction at all.

(10) Saltiel, G.; D'Agostino, J.; Megarity, E. D.; Metts, L.; Neuberger, K. R.; Wrighton, M.; Zafiriou, O. C. *Org. Photochem.* **1973**, *3*, 1.

The first case is represented by the *(E)* furylidenoxindole **1a**. Following the classification proposed by Schmidt[1,2] for photochemical dimerizations, the crystal packing of this compound is of the α type: (i) The distance between parallel molecules related by a lattice translation is quite long (5.523 Å), because of the large angle $\varphi = 52.5°$ between the translation vector and the normal to the molecular planes. (ii) Instead, the pairs of molecules related by an inversion center face each other in a head−tail arrangement (Figure 4b) favorable to photoreaction, with a distance between the double bonds of only 3.498 Å (cf. Table 2 for the other geometrical parameters foreseen by the topochemical rules). Only van der Waals forces and weak C−H···O interactions held together the molecules. Acetylation of the indole nitrogen prevents the formation of stronger interactions via the N−H group.[11]

Indeed, crystals of this substance are highly photoreactive, and the observed cracking of the prismatic crystals in a direction normal to their elongation axis is in keeping with the observed crystal packing. The planes of flat molecules stack one on top of the other along the direction of the short *b* axis, which therefore corresponds to the easiest crystal growth direction (elongation axis). The reacting molecules, approaching each other, move away from the parallel translationally related molecules up to the point of breaking the crystal lattice in the direction perpendicular to the translation. The details of the process have not been fully clarified. The powder diffraction analysis of the product of the cyclophotoaddition of **1a** shows that the "as formed" crystalline dimer has a polymorphic form different from that of the recrystallized sample (the crystal structure of which has been determined). To determine the crystal structure of the "as formed" dimer, which may be considered as an intermediate step of the process, we collected the high resolution powder diffraction pattern at the ESRF synchrotron source. So far, all our attempts at indexing the pattern have failed, probably because the sample contains more than one crystalline phase.

The fact that dibenzylidenecyclopentanone, a molecule that bears some resemblance to the present derivatives, yields a photodimer as an "amorphous" phase rather than undergoing a crystal-to-crystal transformation has been previously rationalized[8] as being due to the fact that the intrinsic rigidity of this large molecule precludes that the dimer fits into the monomer lattice, as is possible with smaller or more flexible derivatives, and at any rate that the formation of new products disrupts the arrangement of the crystals.[12] The similar rigidity of **1a** may be the cause of our failure to carry out single crystal to single crystal reaction upon irradiation into the outermost absorption flank.[3−5]

As for the *(E)* phenylidene derivative **1b**, the arrangement of the molecules in the crystal is again of the α type, with $\varphi = 62.0°$ and translation distance of 8.10 Å, while the two head-to-tail faced molecules related by the inversion center (Figure 5b) are much closer and in a topochemically favorable arrangement (Table 2), even though the distance between the two double bonds (3.877 Å) is slightly larger than in **1a**. The twist of the phenyl ring can be due to steric hindrance with the neighboring ring and/or energy gain in crystal packing. Indeed, the twist allows a favorable interaction between one of the phenyl protons and the π cloud of the six-membered ring of the oxindole system of the facing molecule, as shown in Figure 5b.

Despite the favorable molecular arrangement, no topochemical photocycloaddition takes place with **1b**. The quantum yield for conversion is $\ll 10^{-2}$, and the products formed (a mixture of dimers, some polymeric material) may arise from reactions at defects rather than being lattice-determined. The reason for the difference between the two *(E)* arylidene derivatives **1a** and **1b** is not apparent at first sight, because both compounds display the same α crystal packing and satisfy the topochemical requirements as far as distance and parallelism of the relevant C=C bond are concerned, even though the distance is slightly (by 0.378 Å) larger for the unreactive benzylidene derivative. The most relevant difference found in the crystal structures is the different planarity of the molecules and thus the lesser degree of "stilbene-type" conjugation in the phenyl derivative.

Molecular packing in the crystal may play a role. From a qualitative point of view, one may notice that, according to the rules proposed by Kitaigorodski,[13] the packing of the benzylidene derivative **1b**, crystallizing in the ubiquitous $P2_1/c$ space group, should be more compact than that of the furylidene derivative **1a**, crystallizing in the rarer $P2/n$ space group with less translational symmetry. The values of the calculated densities seem to point in the opposite direction, but the difference is small. A more quantitative estimate of the packing effects was attained from the charge density estimation of the molecular interaction energies. Indeed, the cohesion energy was 2 kcal/mol smaller for **1a** (−3 kcal/mol) than for **1b** (−5 kcal/mol), and the value of the interaction energy between potentially reactive molecules was 3 kcal/mol larger for **1a** (−4 kcal/mol) than for **1b** (−1 kcal/mol).

We have tried to confirm these results by carrying out ab initio theoretical calculations both on the periodic crystals and on the isolated molecules of **1a** and **1b**. Unfortunately the results on the crystals did not yield interpretable results.[14] The molecular calculations were carried out both on single molecules and on pairs of facing molecules, as in Figures 4b and 5b, to evaluate the interaction energy. Even though these calculations were performed with a variety of methods, the values of the interaction energy turned out to be close to zero, as expected for a purely dispersive interaction. This result is in keeping with the small values of the interaction energy obtained from the charge density analysis. The most significant outcome was the clear indication that the rotation of the phenyl ring in **1b** is mainly due to the steric repulsion between the protons at C6′ and C4, as shown by the value of the twist angle (51.2° in the

(11) These hydrogen bond interactions were indeed found in the crystal structure of 2-benzylidenoxindole, the crystals of which had been obtained in one of our attempts at growing suitable crystals of **2b**. The crystal structure will not be described here, but the data will be deposited with the Cambridge Crystallographic Data Centre, with deposition number CCDC-137079.

(12) This is another case where, despite the fact that the dimer does not fit easily within the structure of the monomer, an important condition according to Kaupp's scheme, the dimerization occurs efficiently (ca 90%) as predicted topochemically, though not in a crystal to crystal way.

(13) Kitaigorodski, A. I. *Organic Chemical Crystallography*; Consultants Bureau, 1961,

(14) The calculated lattice energies for **1a** and **1b** tend to zero or even to positive values. This may be attributed to the known inability of the Hartree−Fock and Density Functional methods to handle weak dispersive interactions. We intend to verify this hypothesis by carrying out calculations on smaller molecular crystals.

isolated molecule and 40.5° in the facing pair). On the other hand, the optimized geometry of the molecule of **1a** becomes completely flat.

The lack of reactivity in the *(E)* benzylidene derivative **1b** can thus be attributed to two connected factors: the twist of the phenyl ring and the greater cohesion of the packing. As for the first factor, apparently a planar 1,2-disubstitued ethylene moiety is required for the reaction (indeed there are no examples of reactive monosubstituted or 1,1-disubstituted ethylenes). Thus, the *(E)* furylidene derivative **1a** undergoes a model photocycloaddition under topochemical control,[2,15] and the excited molecule finds no barrier toward the funnel leading to addition,[16a] as shown by the high quantum yield and absence of luminescence. However, in **1b** a slight torsion of the stilbene moiety introduces a barrier into the path leading to cycloaddition and hinders the reaction. In this case the excited state decays either radiatively (notice that the fluorescence from the solid is similar in shape to that in glassy solution, indicating that the conformation is similar in the two cases) or via a nonradiative internal conversion (as suggested by the fact that the luminescence is weak), which presumably involves a molecular motion initially not dissimilar to that leading to cycloaddition. The small increase in energy in **1b** is counterbalanced by the closer packing, revealed by the larger cohesion energy and mostly due to the phenyl C−H−oxindole ring interaction shown in Figure 5b.

Ariel et al.[16b] have explained the similar lack of photoreactivity observed in 4,4,8α-trimethyl-8aβ-carbomethoxy-4aβ,5,8,8a-tetrahydro-1(4*H*)-naphthalen-1-one as caused by a "steric compression effect" due to a repulsive interaction between methyl hydrogens in different molecules, which, as the reacting molecules approach each other, get so close one to the other as to hinder the possible reaction. In our case the more effective packing is attained also through a favorable C−H···π interaction, and the "steric compression" may be interpreted as the lack of sufficient space for rotation and reaction.

In contrast, the crystal packing for the *(Z)* furylidenoxindole **2a** (and by inference also for **2b**, for which we were unable to grow suitable crystals) corresponds to the unreactive Schmidt's γ form, with the closest molecules separated by the shortest $a = 4.596$ Å lattice translation (Figure 6b), which is too large for the photoreaction to occur. This explains the lack of photocycloaddition for the two *(Z)* derivatives in terms of unsuitable γ crystal packing. Noteworthy, the crystals of these materials exhibit an intense luminescence, which is red-shifted with respect to that observed in a glassy solution at 77 K, possibly due to a more strict planarity of these molecules in the crystalline state (see Figure 6a for **2a**).

Conclusions

With the present study we have been able to rationalize the photochemical behavior of a family of four arylidenoxindole derivatives by comparing the results of a series of crystal structure analyses with those of the photochemical study. On the basis of the topochemical principle[1] alone, applied to the analysis of the crystal structures, it has been possible to explain both the absence of photocycloaddition in the (*Z*) derivative **2a**, which crystallizes in the unreactive γ form, and the high reactivity of the (*E*) furylidene derivative **1a**, which adopts the α form with a very favorable topochemical head−tail facing of the molecules. To explain the unexpected lack of reactivity of the (*E*) benzylidene derivative **1b**, which also adopts the α form with a favorable topochemical head−tail facing of the molecules, a more detailed analysis of the molecular geometry, the weak intermolecular interactions, and the crystal packing had to be carried out. The calculation of the interaction energies from the charge density study on the low-temperature diffraction data proved to be a valuable tool for analyzing these factors. The twist of the phenyl ring with respect to the oxindole moiety, the interaction between a phenyl proton and the π cloud of the six-membered ring in the oxindole nucleus of a facing molecule, the relatively high cohesion energy, and the low interaction energy between facing molecules in the crystal were found to be the main factors preventing photoreaction in the case of **1b**. This points to a further stringent requisite for topochemical dimerizations and suggests that cohesion energy should be taken into account when rationalizing negative results.

A number of problems still remain open. Following the suggestions of a number of recent crystal engineering studies on fluorinated derivatives,[17,18] we also intend to carry out the photoreaction of fluorinated analogues of **1b** and test the capability of fluorine to steer reactivity.

Finally, we think that the mechanisms that are at the basis of these types of solid-state reactions need further attention, especially in the cases in which the topochemical principle is unable to explain the reactivity. Progress in this direction may come from some recent Raman phonon studies,[14,19−22] evidencing the relation between the occurrence of topochemical reactions and lattice−phonon interactions, as well as from the appropriate considerations of the limits imposed by the tightness of crystal packing to the molecular movements necessary for the reaction to take place.[23−27] A very recent study of a solid-state photochromic reaction by first principles molecular dynamics techniques[28] might also open a new way to tackle this kind of problem.

(15) Ghosh, M.; Chakrabarti, S.; Misra; T. N. *J. Phys. Chem. Solids* **1996**, *57*, 1891−1895.
(16) (a) Caldwell, R. A. *J. Am. Chem. Soc.* **1980**, *102*, 4004−4007. (b) Ariel, S.; Askari, S.; Scheffer, J. R.; Trotter, J.; Walsh, L. *J. Am. Chem. Soc.* **1984**, *106*, 5726−5728.
(17) Vishnumurthy, K.; Guru Row, T. N.; Venkatesan, K. *J. Chem. Soc., Perkin Trans. 2* **1996**, 1475−1478. Vishnumurthy, K.; Guru Row, T. N.; Venkatesan, K. *J. Chem. Soc., Perkin Trans. 2* **1997**, 615−619.
(18) Coates, G. W.; Dunn, A. R.; Henling, L. M.; Ziller, J. W.; Lobkovsky, E. B.; Grubbs, R. H. *J. Am. Chem. Soc.* **1998**, *120*, 3641−3649.
(19) Misra, T. N.; Prasad, P. N. *Chem. Phys. Lett.* **1982**, *85*, 381−386.
(20) Ghosh, U.; Misra, T. N. *Bull. Chem. Soc. Jpn.* **1985**, *58*, 2403−2406.
(21) Chakrabarti, S.; Gantait, M.; Misra, T. N. *Proc. Ind. Acad. Sci. (Chem. Sci.)* **1990**, *102*, 165−172.
(22) Ghosh, M.; Chakrabarti, S.; Misra, T. N. *J. Phys. Chem. Solids* **1997**, *59*, 753−757.
(23) Cohen, M. D. *Angew. Chem., Int. Ed. Engl.* **1975**, *14*, 386−393.
(24) Gavezzotti, A. *J. Am. Chem. Soc.* **1983**, *105*, 5220−5225.
(25) Murthy, G. S.; Arjunan, P.; Venkatesan, K.; Ramamurthy, V. *Tetrahedron* **1987**, 43, 1225−1240.
(26) Marubayashi, N.; Ogawa, T.; Hamasaki, T.; Hirayama, N. *J. Chem. Soc., Perkin Trans. 2* **1997**, 1309−1314.
(27) Marubayashi, N.; Ogawa, T.; Hirayama, N. *Bull. Chem. Soc. Jpn.* **1998**, *71*, 321−327.
(28) Irmgard, F.; Marx, D.; Parrinello, M. *J. Phys. Chem.* **1999**, *103*, 7341−7344.

Experimental Section

Materials. The arylidenoxindoles **1** and **2** were prepared according to literature methods,[29] purified by chromatography, and recrystallization from ethanol. The main spectroscopic characteristics are reported below.

(*E*)-1-Acetyl-2,3-dihydro-3-(2-furylmethylene)-2*H*-indol-2-one (1a): ^{1}H NMR [$(CD_3)_3SO$] δ 2.65 (s, 3H), 6.88 (dd, J = 2, 4 Hz), 7.30 (dt, J = 2, 7 Hz), 7.42 (dd, J = 2, 7 Hz), 7.45 (d, J = 4 Hz), 7.55 (s, 1H), 8.25 (dd, J = 2, 7 Hz), 8.27 (d, J = 2 Hz), 8.60 (dd, J = 2, 7 Hz); IR (KBr) 1740, 1695, 1180 cm^{-1}.

(*E*)-1-Acetyl-2,3-dihydro-3-(2-phenylmethylene)-2*H*-indol-2-one (1b): ^{1}H NMR [$(CD_3)_3SO$] δ 2.65 (s, 3H), 7.12 (dt, J = 2, 7 Hz), 7.4 (dt, J = 2, 7 Hz), 7.5−7.75 (m, 5H), 7.85 (s, 1H), 8.2−8.25 (m, 2H); IR (KBr) 1740, 1700, 1170 cm^{-1}.

(*Z*)-1-Acetyl-2,3-dihydro-3-(2-furylmethylene)-2*H*-indol-2-one (2a): ^{1}H NMR [$(CD_3)_3SO$] δ 2.68 (s, 3H), 6.88 (dd, J = 2, 4 Hz), 7.25 (dt, J = 2, 7 Hz), 7.35 (dt, J = 2, 7 Hz), 7.92 (s, 1H), 7.95 (dd, J = 2, 7 Hz), 8.08 (d, J = 2 Hz), 8.15 (d, J = 7 Hz), 8.22 (d, J = 4 Hz); IR (KBr) 1730, 1695, 1160 cm^{-1}.

(*Z*)-1-Acetyl-2,3-dihydro-3-(2-phenylmethylene)-2*H*-indol-2-one (2b): ^{1}H NMR [$(CD_3)_3SO$] δ 2.62 (s, 3H), 7.28 (dt, J = 2, 7 Hz), 7.38 (dt J = 2, 7 Hz), 7.5−7.6 (m, 5H), 7.92 (dd, J = 2, 7 Hz), 8.05 (s, 1H), 8.15 (dd, J = 2, 7 Hz); IR (KBr) 1725, 1695, 1155 cm^{-1}.

Photochemical Reactions in Solution. Solutions (100 mL, 1×10^{-2} M) of the oxindoles **1** and **2** in MeCN were flushed with argon and irradiated by means of a 125 W Pyrex-filtered mercury arc (medium pressure) in an immersion well apparatus at 17 °C. After 1−2 h the steady state *E*/*Z* composition was reached (6/4 to 1/1 mixtures in all cases) as determined by HPLC (on the basis of appropriate calibration curves, by using a Supelcosil LC−SI column and cyclohexane ethyl acetate mixtures as eluants) and NMR of the residue after solvent distillation. Irradiation for up to 10 h produced small amounts of further products (colorless spots in TLC).

Quantum yield measurements were carried out on similar solutions in quartz tubes. These were inserted in a merry-go-round apparatus fitted with eight 15 W phosphor-coated lamps (center of emission, 366 nm). The product formation was followed by HPLC, and the light flux was determined by ferrioxalate actinometry.

Photochemical Reactions in the Solid State. A finely ground sample of compound **1a** (200 mg) was evenly spread on a 5 cm × 20 cm glass plate and exposed to the light from two 15 W phosphor-coated lamps (366 nm) at 10 cm distance. The powder was occasionally mixed. After 10 h, the powder was washed with a little chloroform, dissolving some unreacted starting material. The colorless residue (140 mg) was practically pure dimer **3a**, as shown by the spectra. This could be recrystallized from nitroethane. When large crystals were used, these burst into smaller fragments that were scattered around for several centimeters. The photodecomposition was readily observed by simply leaving the crystals on the bench exposed to natural or artificial light.

2,9-Diacetyl-2,9-diaza-3,4:10,11-dibenzo-6,12-bis-(2-furyl)-dispiro[4.1.4.1]dodecan-1,8-dione (3a): mp 225 °C (nitroethane, with decomposition; monomeric **1a** was a product). Anal. Found: C, 71.1; H, 4.2; N, 5.4. Calcd for $C_{15}H_{11}NO_3$: C, 71.14; H, 4.37, N, 5.53. ^{1}H NMR [$(CD_3)_3SO$] δ 2.52 (s, 3H), 4.78 (s, 1H), 5.72 (d, J = 4 Hz), 6.28 (dd, J = 2, 4 Hz), 7.42 (dd, J = 2, 7 Hz), 7.47 (d, J = 2 Hz), 7.48 (dt, J = 2, 7 Hz), 8.02 (dd, J = 2, 7 Hz), 8.18 (dd, J = 2.7 Hz). IR (KBr) 1755, 1710, 1275, 1170 cm^{-1}.

The quantum yield of reaction was measured by mixing and grinding 2.5 mg of **1a** with 250 mg of KBr and exposing the synthesized pellet to the light from a focused 150 W high-pressure mercury arc fitted with an interference filter (transmission peak at 366 nm). Under these conditions, light was completely absorbed by the sample. IR spectra were registered. After 2, 4, and 6 min of irradiation the pellets were dissolved in water and extracted with ethyl acetate, and the organic phase was analyzed by HPLC. A similar reaction was carried out on identically prepared KBr pellets containing 2 mg of 2-nitrobenzaldehyde, which was taken as an actinometer (Φ = 0.5).[9]

The photochemistry of the other oxindoles was similarly investigated. Irradiation of **1b** (7 days) gave a highly insoluble material. Part of this could be dissolved in DMSO and analyzed by NMR. Besides unreacted **1b**, it contained only traces (ca. 10% overall) that were suggestive of dimers, since separate signals for the acetyl group and the cyclobutyl protons (in the δ 5−5.5 region) were detected. The insoluble part showed a IR band at 1760 cm^{-1}.

Similar irradiation of **2a** (7 days) also showed formation of bands at 1760 cm^{-1}. The photolyzed crystals could be dissolved for the main part in DMSO and analyzed by NMR. Signals attributed to two dimers could be detected in the spectrum of the mixture. The signals attributed to the acetyl, cyclobutyl, and two of the furyl ring signals were as follows: main product δ 2.62, 4.87, 5.52, 6.35; minor 2.58, 4.87, 5.33, 6.20. Two other isomers were present in trace, as deduced from similar but less intense signals. Overall the dimers amounted to ca. 25% of the starting oxindole. Attempted chromatographic separation was unsuccessful.

X-ray Analyses. Crystals of **1a**, **1b**, **2a**, and **3a** suitable for X-ray analysis were obtained by slow evaporation of ethanol solutions. The diffraction experiments were carried out at 150 K for all derivatives except **2a**, which did not give good enough crystals. Crystallographic data and details of data collections and refinements are given in Table 1. Data reduction was carried out by the Siemens P3/PC program,[30] and Lorentz and polarization corrections were performed. No absorption correction was applied. The structures were solved by direct methods using the SIR97 program[31] and refined using the SHELXTL/IRIS[32] and the SHELXL-97[33] programs. The refinement was by least-squares full matrix method, with anisotropic displacement parameters for all non-hydrogen atoms. The hydrogen atoms were located in calculated positions and treated as riding atoms during the refinement.[34]

Powder diffraction experiments were carried out on a Siemens D-5000 diffractometer using Cu Kα radiation (λ = 1.54178 Å). The powder pattern of the "as obtained" dimer **3a** was collected at the beamline BM-16 of the European Synchrotron Radiation Facility in Grenoble (France).

Charge Density Analyses. Since the diffraction data of **1a** and **1b** extended to sin θ/λ = 0.6513 and 0.8076 Å^{-1} respectively, the analyses were carried out using only the monopole model, within the aspherical-atom formalism developed by Stewart[35] and implemented in the VALRAY set of programs.[36] The two monopoles of each C, N, and O atom were derived from the canonical SCF s- and p-orbitals.[37] The outer monopole was shaped with a variable scaling parameter k, describing the contraction/expansion of the spherical compo-

(29) Tacconi, G.; Marinone, F. *Ric. Sci.* **1968**, *38*, 1239−1244. Stanek, J.; Ryber, D. *Chem. Listy* **1946**, *40*, 173−190. Tacconi, G.; Marinone, F.; Desimoni, G. *Gazz. Chim. Ital.* **1971**, *101*, 173−182.

(30) *P3/PC Diffractometer Program*, Version 3.13; Bruker Analytical X-ray Instruments Inc.: Madison, WI; 1989.

(31) Altomare, A.; Burla, M. C.; Camalli, M.; Cascarano, G.; Giacovazzo, C.; Guagliardi, A.; Moliterni, A. G.; Polidori, G.; Spagna, R. *J. Appl. Crystallogr.* **1999**, *32*, 115−119.

(32) Sheldrick, G. M. *SHELXTL/IRIS*; Bruker Analytical X-ray Instruments Inc.: Madison, WI, 1990.

(33) Sheldrick, G. M. *SHELXL-97*; University of Göttingen: Gottingen Germany, 1997.

(34) Supporting Information (atomic coordinates, anisotropic thermal parameters, bond distances and angles) has been deposited with the Cambridge Crystallographic Data Centre, with deposition numbers CCDC-137080 for **1a**, CCDC-137077 for **1b**, CCDC-137076 for **2a**, and CCDC-137078 for **3a**.

(35) Stewart, R. F. Electrostatic properties of molecules from diffraction data. In *The Application of Charge Density Research to Chemistry and Drug Design*; Jeffrey, A., Piniella, J. F., Eds.; Plenum Press: New York, 1991; p 63 and references therein.

(36) Stewart, R. F.; Spackman M. A., *VALRAY users's manual*; Department of Chemistry, Carnegie-Mellon University: Pittsburgh, 1983.

(37) Clementi, E.; Roetti, C. *At. Data Nucl. Data Tables 14* **1974**, 177−148.

nent of the valence electron density.[38] The H atom monopole was expressed by the radial function exp(−2.48*r*). The calculation of the molecular interaction energies was carried out using the model proposed by Spackman et al.[39−40]

Theoretical Calculations. For our attempt at calculating the lattice energy of the crystals by the ab initio Hartree−Fock (HF) method, we have employed the CRYSTAL98[41] program. Ab initio Hartree−Fock (HF) and Density Fuctional (DFT) SCF-MO calculations were performed using the Gaussian98[42] program. The initial geometry was the one obtained from the X-ray analysis, and the geometry optimization was carried out, at HF level, using 6-31G(d,p) and/or 6-31G(d)[43] basis sets. Single point Becke3LYP DFT calculations were performed on the above optimized geometries to obtain more accurate estimates of their relative energy.

The graphic analysis was mainly performed using the MOLDRAW program.[44]

Acknowledgment. We wish to thank Dr. Paolo Redana for his valuable contribution to this work in the initial stages and Prof. Vincenzo Massarotti and Dr. Doretta Capsoni for carrying out some of the powder diffraction experiments.

JO991873I

(38) van der Wal, R. J.; Stewart, R. F. *Acta Crystallogr*. **1984**, *A40*, 587−593.

(39) Spackman, M. A. *J. Chem. Phys.* **1986**, *85*, 6579−6586.

(40) Spackman, M. A.; Weber H. P.; Craven B. M. *J. Am. Chem. Soc*, **1988**, *110*, 775−782.

(41) Saunders, V. R.; Dovesi, R.; Roetti, C.; Causà, M.; Harrison, N. M.; Orlando, R. Zicovich-Wilson C. M. *CRYSTAL98, Version 1.0, User's Manual*; 1999.

(42) Frisch, M. J.; Trucks, G. W.; Schlegel, H. B.; Scuseria, G. E.; Robb, M. A.; Cheeseman, J. R.; Zakrzewski, V. G.; Montgomery, J. A., Jr.; Stratmann, R. E.; Burant, J. C.; Dapprich, S.; Millam, J. M.; Daniels, A. D.; Kudin, K. N.; Strain, M. C.; Farkas, O.; Tomasi, J.; Barone, V.; Cossi, M.; Cammi, R.; Mennucci, B.; Pomelli, C.; Adamo, C.; Clifford, S.; Ochterski, J.; Petersson, G. A.; Ayala, P. Y.; Cui, Q.; Morokuma, K.; Malick, D. K.; Rabuck, A. D.; Raghavachari, K.; Foresman, J. B.; Cioslowski, J.; Ortiz, J. V.; Baboul, A. G.; Stefanov, B. B.; Liu, G.; Liashenko, A.; Piskorz, P.; Komaromi, I.; Gomperts, R.; Martin, R. L.; Fox, D. J.; Keith, T.; Al-Laham, M. A.; Peng, C. Y.; Nanayakkara, A.; Gonzalez, C.; Challacombe, M.; Gill, P. M. W.; Johnson, B.; Chen, W.; Wong, M. W.; Andres, J. L.; Gonzalez, C.; Head-Gordon, M.; Replogle, E. S.; Pople, J. A. *Gaussian 98, Revision A.7*; Gaussian, Inc.: Pittsburgh, PA, 1998.

(43) Hehre, W. J.; Radom, L.; Schleyer, P.v.R.; Pople, J. A. *Ab initio molecular orbital theory*, 1st ed.; John Wiley & Sons: New York, 1986; Chapter 4.

(44) Ugliengo, P.; Viterbo, D.; Chiari, G. *Z. Kristallogr*. **1993**, *207*, 9−23. Available at http://www.ch.unito.it/ifm/fisica/moldraw/moldraw.html.